Nonlinear equilibration of two-dimensional optimal perturbations in viscous shear flow

Kathryn M. Butler[a] and Brian F. Farrell
Division of Applied Sciences, Harvard University, Cambridge, Massachusetts 02138

(Received 7 July 1993; accepted 24 February 1994)

Two-dimensional perturbations configured for maximum energy growth in laminar viscous shear flow are shown to develop into quasisteady finite amplitude structures, provided that the initial perturbation has sufficient energy and a nearby nonlinear mode exists. For Poiseuille flow, which supports finite amplitude equilibria for Reynolds numbers above ~2900, an optimal perturbation with initial energy density equal to or greater than 0.1% of the mean flow energy density closely approaches the quasiequilibrium state within 10 advective time units. For Couette flow, which has no finite amplitude solution, the optimal perturbations decay rapidly after reaching maximum amplitude unless the configuration is sufficiently close to a linear mode with slow exponential decay rate. While the quasiequilibrium structure for Poiseuille flow is locally inflectional, it supports only weak instabilities with scales larger than the local region.

I. INTRODUCTION

Nonlinear coherent structures play an important role in many aspects of fluid behavior. Vibrating ribbons are commonly used to generate a coherent two-dimensional (2-D) flow field in forced transition experiments such as those of Klebanoff *et al.*[1] and Nishioka *et al.*[2] Secondary instability theories,[3,4] rely on these 2-D structures to support three-dimensional (3-D) parametric secondary instabilities.

The problem of the origin of coherent structure from the background flow field is a central theoretical issue that has received little attention. For stable basic flows with strong forcing, such as those alluded to above, the origin can be related to the forcing. When a strong coherent forcing is not imposed, the problem of identifying the source of the coherent structure is more difficult.

In plane Poiseuille flow, a finite amplitude quasiequilibrium state can arise from the development of 2-D disturbances. The unperturbed Poiseuille flow is linearly unstable (albeit with small growth rates) for Reynolds numbers above $R_c=5772$ (Ref. 5) based on channel half width and centerline velocity and supports up to two finite amplitude nonlinear solutions at a given streamwise wave number α for $R\gtrsim 2900$. Taking E to be the finite amplitude perturbation energy density, the neutral surface representing this set of subcritical and supercritical finite amplitude equilibria, mapped out in (E,R,α) space by Zahn *et al.*[6] and Herbert,[7] has been shown by Orszag and Patera[8] to attract 2-D modal disturbances above a threshold energy for Reynolds numbers as low as $R\sim 1000$. The evolution of these finite amplitude modal disturbances toward the equilibrium point follows a route characterized by two time scales: the eddy circulation time $1/\sqrt{E}$ (of order 10) over which the initial flow develops into a quasiequilibrium state, and the viscous time scale R over which the flow develops along a band of quasiequilibria toward the steady solution.

Plane Couette flow differs from Poiseuille flow in that it supports neither exponentially growing modes nor (apparently) 2-D finite amplitude equilibria (although it does support 3-D equilibria[9]). In order to demonstrate the growth of 3-D secondary instabilities on 2-D quasiequilibria for Reynolds numbers down to $R\sim 1000$ based on channel half width and upper wall velocity, Orszag and Patera[10] found it necessary to superimpose a large amplitude 2-D modal disturbance on the basic flow. An initial perturbation of $E_1\approx 4\%\ \bar{E}$, where $\bar{E}$ is the mean flow energy density, gives the 3-D secondary instabilities sufficient time to develop on the rapidly decaying 2-D structures.

Clearly it would be useful to identify initial conditions that are particularly effective at converting a nearly parallel flow into a flow containing long-lasting finite amplitude structures. In particular, for the secondary instability mechanism to explain the onset of natural transition in subcritical flows, a long-lasting 2-D elliptical structure must somehow arise from low levels of background noise.

A general approach to the question of the origin of finite amplitude disturbances has been proposed by Farrell,[11] who demonstrated that properly configured initial conditions that are not of exponential modal form can grow rapidly (on the advective time scale) by tapping the kinetic energy available in the mean shear. In this paper, we follow the nonlinear development of 2-D perturbations that are optimally configured in the linear problem to gain the most energy. The tendency of these initial disturbances to evolve nonlinearly into quasisteady structures is investigated for both Poiseuille and Couette flows. Using the criteria provided by Landman and Saffman[12] on the 3-D instability of a 2-D elliptical vortex, we estimate the initial disturbance energy required to initiate transition. We also compare the growth of exponential instability suggested by the inflectional nature of local profiles within the quasiequilibrium flow with the growth arising from optimal perturbation of the 2-D structures.

II. NONLINEAR EVOLUTION OF A TWO-DIMENSIONAL FLOW

The Navier–Stokes and continuity equations for an incompressible two-dimensional viscous flow are

[a]Present address: Building and Fire Research Laboratory, NIST, Gaithersburg, Maryland 20899.

 1070-6631/94/6(6)/2011/10/$6.00

$$\frac{\partial u}{\partial t}+u\frac{\partial u}{\partial x}+v\frac{\partial u}{\partial y}=-\frac{\partial p}{\partial x}+\frac{1}{R}\Delta u, \tag{1a}$$

$$\frac{\partial v}{\partial t}+u\frac{\partial v}{\partial x}+v\frac{\partial v}{\partial y}=-\frac{\partial p}{\partial y}+\frac{1}{R}\Delta v, \tag{1b}$$

$$\frac{\partial u}{\partial x}+\frac{\partial v}{\partial y}=0, \tag{1c}$$

where $\Delta\equiv(\partial^2/\partial x^2+\partial^2/\partial y^2)$. The two-dimensional continuity equation enables us to define a streamfunction ψ, such that $u\equiv-\partial\psi/\partial y$ and $v\equiv\partial\psi/\partial x$. Eliminating the pressure p from the Navier–Stokes equations results in the vorticity/streamfunction formulation

$$\frac{\partial q}{\partial t}+J(\psi,q)=\frac{1}{R}\Delta q, \tag{2a}$$

$$q=\Delta\psi, \tag{2b}$$

with $J(\psi,q)\equiv(\partial\psi/\partial x)(\partial q/\partial y)-(\partial\psi/\partial y)(\partial q/\partial x)$.

Suitable boundary conditions for channel flow are no slip at the walls located at $y=\pm1$ and periodic in the streamwise (x) direction

$$\frac{\partial\psi}{\partial x}(x,\pm1,t)=0, \tag{3a}$$

$$\frac{\partial\psi}{\partial y}(x,\pm1,t)=-U_{\pm1}, \tag{3b}$$

$$\psi(0,y,t)=\psi(a,y,t), \tag{3c}$$

where $a=2\pi/\alpha$ is the x wavelength. For Couette flow, the flow rate is fixed by making $\psi(\pm1,t)$ constant. For Poiseuille flow, the mean pressure gradient is assumed constant, and integration of Eq. (1a) over both x and y results in a time dependence of ψ at each wall that can be written as

$$\begin{aligned}\frac{\partial\psi}{\partial t}(1,t)&=P'-\frac{1}{R}\frac{\overline{\partial u}}{\partial y}(1,t),\\ \frac{\partial\psi}{\partial t}(-1,t)&=-P'-\frac{1}{R}\frac{\overline{\partial u}}{\partial y}(-1,t).\end{aligned} \tag{4}$$

Here an overbar indicates an average in x and P' is the fixed pressure gradient. Boundary condition (3b) is turned into a constraint on vorticity q using the second-order Pearson's approximation.

The perturbation can be expressed in a reference frame traveling with velocity c_{ref} in the streamwise direction by modifying the streamfunction

$$\psi\Rightarrow\psi+c_{\text{ref}}y. \tag{5}$$

In order to view the emergence of a quasiequilibrium state, the reference velocity is selected to hold the nonlinear structure approximately steady in the x direction.

The vorticity equation is approximated numerically using a Fourier spectral method in x and finite differences in y. The advective term is represented by third-order Adams–Bashforth scheme, and the solution is stepped in time according to the Crank–Nicolson scheme. Convergence properties are second order in both time and space. Depending on the initial conditions, the size of the problem may be reduced by a factor of 2 using symmetry about the $y=0$ axis. The numerics were verified by integrating Orr–Sommerfeld waves of infinitesimal amplitude forward in time to check velocity and growth rate against known values.

The discretization used was $N_x=33$ and $N_y=201$ (halved using symmetry) for Poiseuille flow at $R=4000$, and $N_x=33$ and $N_y=151$ for Couette flow at $R=1000$. The accuracy of this discretization was tested by performing short integrations with double the number of nodes in x or y directions. In each case ratios of perturbation energy to total energy over time agreed within roughly 5%.

III. LINEAR OPTIMAL PERTURBATIONS

Farrell[11] suggests that optimal perturbations of sufficiently high initial amplitude may be particularly disruptive to laminar flow. These disturbances are set up for use as initial conditions for the nonlinear dynamic equations in the following manner.

We start by linearizing the vorticity equation, letting

$$\psi(x,y,t)=\Psi(y)+\psi'(x,y,t), \tag{6}$$

with mean flow velocity $U(y)=-d\Psi/dy$. The perturbations of interest are periodic in the x direction, so solutions are sought in the form

$$\psi'=\tilde{\psi}(y)e^{i\alpha(x-ct)}. \tag{7}$$

Substituting Eqs. (6) and (7) into the vorticity equation (2) results in the Orr–Sommerfeld equation

$$\begin{aligned}&\mathscr{L}\tilde{\psi}=c\tilde{\psi},\\ &\mathscr{L}=\Delta^{-1}\left(U\Delta-U''-\frac{\Delta\Delta}{i\alpha R}\right),\end{aligned} \tag{8}$$

where $\Delta\equiv(d^2/dy^2-\alpha^2)$. The no-slip boundary conditions for channel flows, including plane Poiseuille and Couette flows, become

$$\tilde{\psi}(\pm1)=\frac{\partial\tilde{\psi}}{\partial y}(\pm1)=0. \tag{9}$$

The spectrum of modes for bounded flows is both discrete[13] and complete.[14,15] Therefore, the evolution of an arbitrary initial disturbance $\tilde{\psi}e^{i\alpha x}$ in time can be expressed as an infinite sum of modes

$$\psi'=\sum_{j=1}^{\infty}\gamma_j(\tilde{\psi}_j e^{-i\alpha c_j t})e^{i\alpha x}, \tag{10}$$

where the set of coefficients γ_j is the spectral projection. In practice this sum is truncated at some number of modes, N, sufficient to capture the behavior of interest, so that Eq. (10) can be written in matrix form as

$$\psi'=\mathbf{S}_\tau\boldsymbol{\gamma}e^{i\alpha x}. \tag{11}$$

Here $\mathbf{S}_\tau$ is a matrix whose columns are the discretized approximation to the Orr–Sommerfeld eigenvectors each moved forward by time τ.

If $\mathscr{L}$ in Eq. (8) were a normal operator, then the associated quadratic norm could be resolved into noninteracting

contributions from individual orthogonal modes. The development of small disturbances in a viscous shear flow is made more interesting by the fact that the Orr–Sommerfeld operator $\mathscr{L}$ is non-normal in the energy norm

$$\frac{1}{8a}\int_{-1}^{1}\int_{0}^{a}(\nabla\psi'^{*}\cdot\nabla\psi')dx\,dy. \tag{12}$$

This norm is derived from the physical velocities

$$u'=-\frac{1}{2}\left(\frac{\partial\psi'}{\partial y}+\frac{\partial\psi'^{*}}{\partial y}\right),$$
$$v'=\frac{1}{2}\left(\frac{\partial\psi'}{\partial x}+\frac{\partial\psi'^{*}}{\partial x}\right), \tag{13}$$

where the superscript (*) denotes the complex conjugate.

As a result of the non-normality of $\mathscr{L}$, certain combinations of the nonorthogonal eigenfunctions may demonstrate significant transient energy growth. The initial configuration that gains maximum energy is therefore of interest. Substituting for ψ' from Eq. (11) and integrating over x and y provides the energy density at time τ in discretized form as

$$\mathscr{E}(\tau)=\frac{\Delta y}{8}\left(\gamma^{*}\frac{\partial\mathbf{S}_{\tau}^{*}}{\partial y}\frac{\partial\mathbf{S}_{\tau}}{\partial y}\gamma+\alpha^{2}\gamma^{*}\mathbf{S}_{\tau}^{*}\mathbf{S}_{\tau}\gamma\right)=\gamma^{*}\mathbf{A}_{\tau}\gamma. \tag{14}$$

The matrix $\mathbf{A}$ is Hermitian, and defines a positive definite quadratic form on the spectral projection γ. The linear perturbation that results in maximum energy at time τ given unit initial energy can be found through a variational problem whose functional is

$$F=\gamma^{*}\mathbf{A}_{\tau}\gamma+\lambda(\gamma^{*}\mathbf{A}_{0}\gamma-1), \tag{15}$$

where λ is the Lagrange multiplier for the fixed initial energy. Setting the first variation in γ to zero results in the Euler–Lagrange equation for this functional,

$$\mathbf{A}_{\tau}\gamma+\lambda\mathbf{A}_{0}\gamma=0. \tag{16}$$

This is a generalized eigenproblem whose eigenvalues λ are the ratios of energy at time τ to energy at time zero corresponding to eigenvectors γ, the spectral projections of the perturbations associated with λ. Arranging the spectra in order of decreasing eigenvalue λ orders the necessarily orthogonal initial perturbations by growth over time τ.

Another initial condition that may provide insight into the development of equilibrium flow states is the perturbation that optimally excites a given Orr–Sommerfeld mode. Of particular interest is the least-rapidly decaying mode that, given sufficient time, will come to dominate the perturbation field in the initial value problem. As shown by Farrell,[11] this initial condition is obtained from the variational problem whose functional is

$$F=\gamma^{*}\mathbf{A}_{0}\gamma+\lambda(\gamma\cdot\boldsymbol{\epsilon}_{1}-1), \tag{17}$$

where $\boldsymbol{\epsilon}_{1}$ is the unit column vector that selects the least-rapidly decaying mode. Requiring stationarity in γ results in the Euler–Lagrange equation

$$\mathbf{A}_{0}\gamma=-\lambda\boldsymbol{\epsilon}_{1}, \tag{18}$$

which gives us the optimal spectral projection of

$$\gamma=-\lambda\mathbf{A}_{0}^{-1}\boldsymbol{\epsilon}_{1}, \tag{19}$$

where λ is chosen to set $\gamma_{1}=1$. Note that time dependence does not enter into this problem; the subscript on matrix $\mathbf{A}_{0}$ is retained for consistency.

Physically, perturbations gain energy through the transport of momentum down the mean momentum gradient mediated by the perturbation Reynolds stress, as indicated by the inviscid energy density equation

$$\frac{\partial\mathscr{E}}{\partial t}=-\frac{1}{2}\int_{-1}^{1}U'\overline{u'v'}\,dy, \tag{20}$$

where the overbar indicates an average in x. A visual indication of the direction of energy transfer for 2-D perturbations can be obtained by observing that the perturbation energy increases when

$$\frac{\partial\psi}{\partial x}\frac{\partial\psi}{\partial y}U'=\left(\frac{\partial\psi/\partial x}{\partial\psi/\partial y}\right)\left(\frac{\partial\psi}{\partial y}\right)^{2}U'=-\left(\frac{\partial y}{\partial x}\right)_{\psi}\left(\frac{\partial\psi}{\partial y}\right)^{2}U' \tag{21}$$

is positive over the integral. As perturbation streamlines oriented with an initial up-shear phase tilt, $(\partial y/\partial x)_{\psi}U'<0$, are advected by the mean shear, the perturbation gains energy. If the mean shear continues to advect the disturbance until the

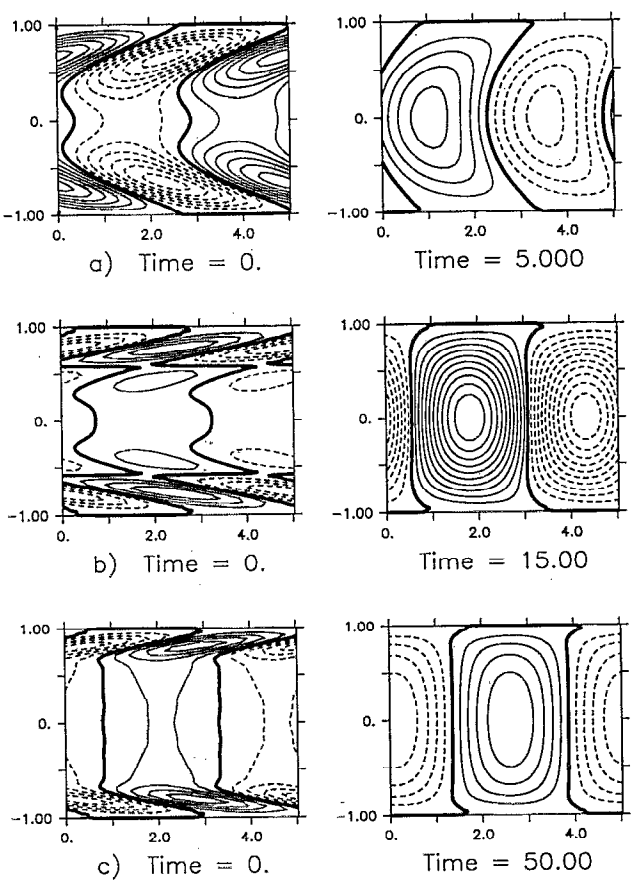

FIG. 1. Energy optimals in Poiseuille flow with $R=4000$, $\alpha=1.25$ for growth times (a) $\tau=5$, (b) $\tau=15$, and (c) $\tau=50$ resulting in energy growth at time τ of $E_{\tau}/E_{0}=7.8$, 35.2, and 9.2, respectively. Streamline contour intervals at $t=\tau$ are 10 times those at $t=0$.

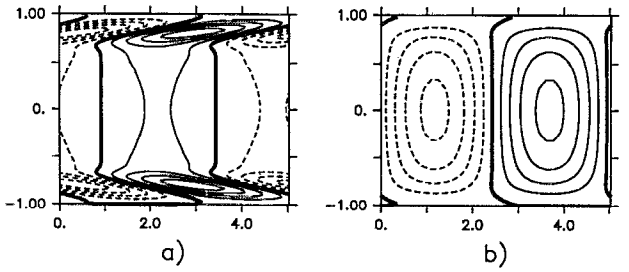

FIG. 2. (a) Streamlines of the conjugate of the differential adjoint eigenfunction, the optimal energy norm configuration for (b) the least stable eigenmode in Poiseuille flow with $R=4000$. Compare with Fig. 1(c).

phase tilt assumes the opposite orientation, indicated by $(\partial y/\partial x)_{\psi}U'>0$, energy is returned to the mean flow by upgradient Reynolds stress.

The complex non-normal eigensystem to find the modes of the Orr–Sommerfeld equation and the generalized Hermitian eigensystem to find the optimal spectral projection are each solved using the QR algorithm. A nine-point difference approximation for the Orr–Sommerfeld operator was selected by verification with the eigenvalues obtained by Orszag[5] for Poiseuille flow.

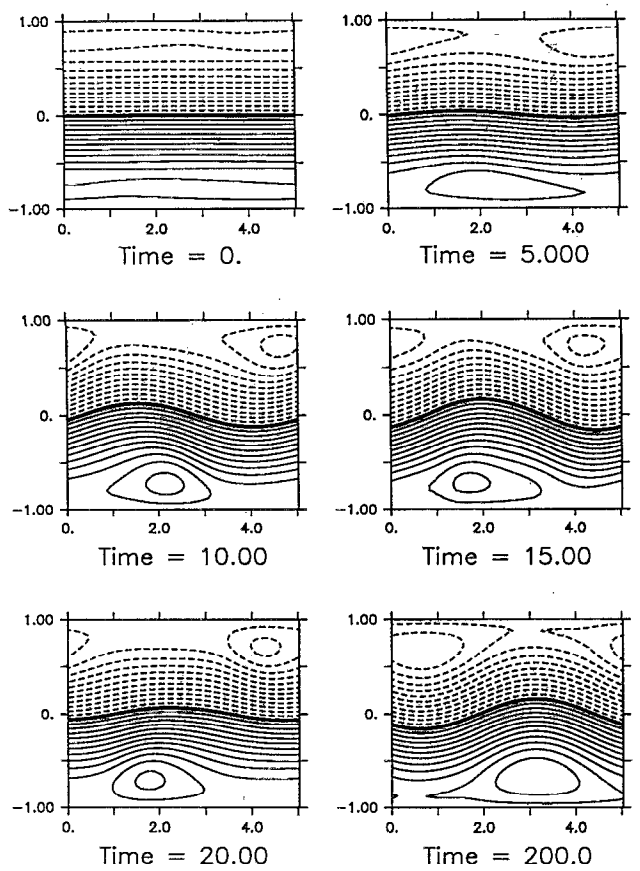

FIG. 3. Nonlinear evolution of the total streamfunction ψ for the 2-D energy optimal in Poiseuille flow with $R=4000$, $\alpha=1.25$, $\tau=15$, and initial perturbation energy $\mathscr{E}_0'=0.1\%\ \overline{\mathscr{E}_0}$ showing the rapid evolution of an elliptical vortex from nearly parallel flow. The reference frame is moving with velocity $c_{\mathrm{ref}}=0.365$.

IV. EQUILIBRATION IN POISEUILLE FLOW

The Navier–Stokes equations admit two-dimensional finite amplitude solutions for Poiseuille flow with Reynolds numbers as low as ~2900. Orszag and Patera[8] demonstrated that the upper branch solution acts as an attractor for finite amplitude disturbances. In their numerical experiments, least rapidly decaying Orr–Sommerfeld modes with initial energy densities above a threshold of 0.1%–0.2% of the mean flow energy density evolved on an advective time scale to a quasiequilibrium state. Further modifications of the flow toward the equilibrated solution occurred only on the much longer diffusive time scale, of order R.

In this section, we explore the nonlinear development of 2-D perturbations that at infinitesimal amplitude are optimally configured to gain maximum energy over a specified time period before their eventual decay. Of particular interest is the tendency of these initial disturbances to evolve into a quasiequilibrium state, the rapidity of this evolution, and the initial energy required to instigate traversal of the path toward equilibration rather than toward linear decay. The wave number selected for study is $\alpha=1.25$ at Reynolds number $R=4000$ so that results may be compared with those of Orszag and Patera. At this Reynolds number no unstable mode is supported.

Figure 1 illustrates the linear development of energy optimals for Poiseuille flow, showing energy growth maxi-

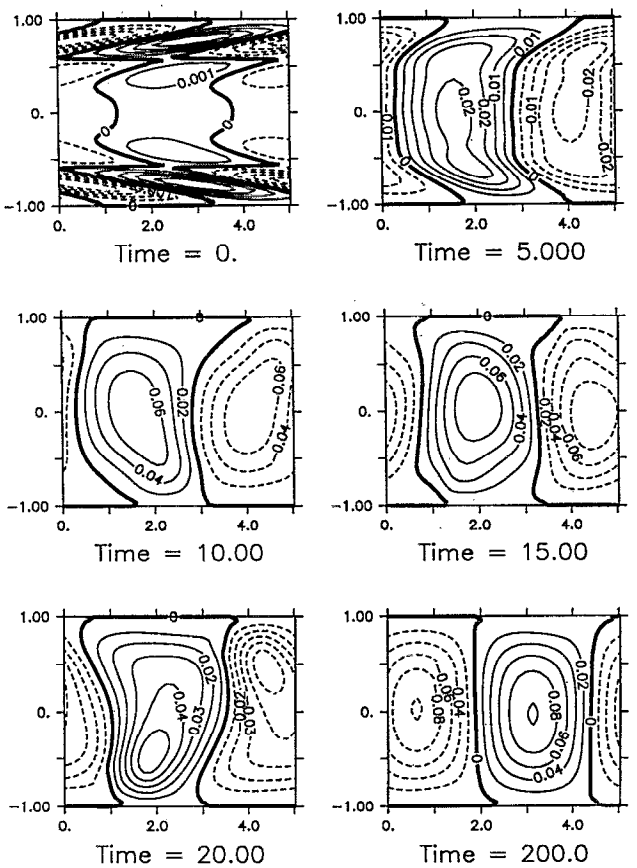

FIG. 4. Evolution of the perturbation streamfunction ψ' for the flow in Fig. 3.

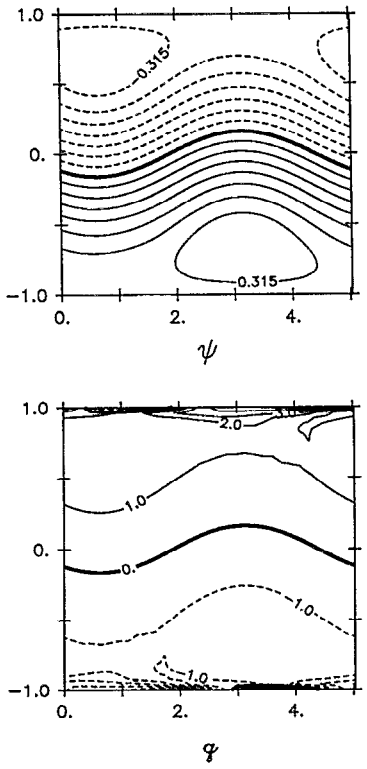

FIG. 5. Total streamfunction and vorticity contours for the quasiequilibrium state at $t=200$ showing parallelism in the interior.

mized over three different growth periods, τ. Note that there is a τ that gives the largest growth in energy. The optimal perturbations for smaller periods do not have time to realize their full growth potential. As the time allotted for energy growth increases, the initial up-shear tilt of the optimal increases to provide more down-gradient Reynolds stress, until viscous damping of these small perturbation scales limits their ability to contribute to energy growth. The optimal perturbation for energy growth at large times [see Fig. 1(c)] is the same as the perturbation that optimally excites the slowest-decaying mode because this mode clearly dominates the perturbation field in the limit $\tau\to\infty$. This optimal can be shown to be the appropriate adjoint of the least damped mode (see Fig. 2).[11] For $R=4000$ and $\alpha=1.25$, the growth period that maximizes the energy growth of an initial perturbation is $\tau\approx 15$, at which time maximum transient growth (in the linear case) of $E_\tau/E_0=35.2$ is obtained. We will investigate the nonlinear evolution of this initial condition. (We note in passing that the 2-D perturbation capable of the largest transient growth with $R=4000$ has a wave number of $\alpha=1.5$ and grows by a factor of 38 in 13 time units.)

The time evolution of this optimal perturbation, assigned an initial energy of 0.1% of the energy in the mean Poiseuille flow ($\overline{E_0}$), is shown in Figs. 3 and 4, in which total and perturbation streamfunctions, respectively, are displayed from a frame of reference traveling with the disturbance. This perturbation rapidly falls into a quasiequilibrium state (Fig. 5) similar to the 2-D finite amplitude solution from

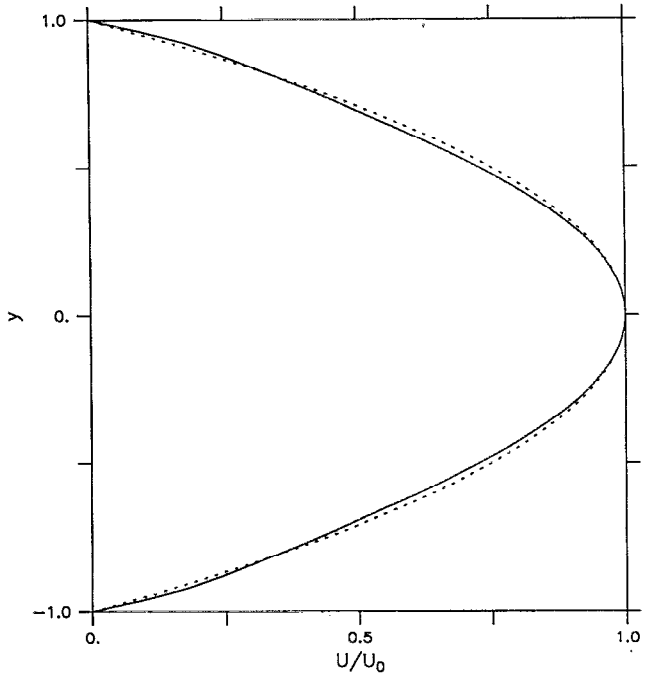

FIG. 6. Mean velocity profile for the quasiequilibrium state at $t=200$ (solid line) relative to the initial Poiseuille profile (dotted line).

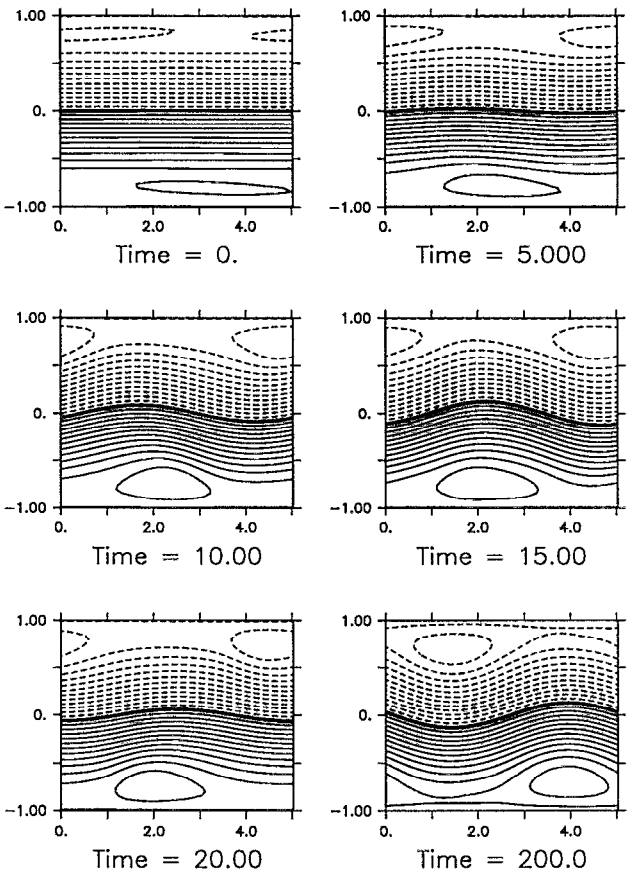

FIG. 7. Nonlinear evolution of the total streamfunction for the 2-D energy optimal in Poiseuille flow with $R=4000$, $\alpha=1.25$, $\tau=15$, and initial perturbation energy $\mathscr{E}_0'=0.05\%\ \overline{\mathscr{E}_0}$. The reference frame is moving with velocity $c_{\text{ref}}=0.35$.

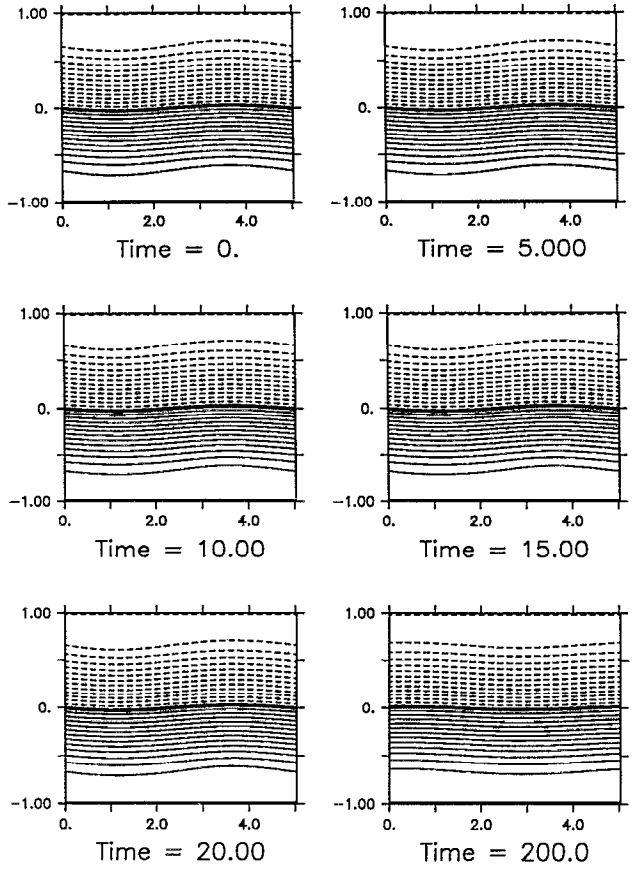

FIG. 8. Nonlinear evolution of the total streamfunction for the slowest-decaying Orr–Sommerfeld mode in Poiseuille flow with $R=4000$, $\alpha=1.25$, and initial perturbation energy $\mathscr{E}_0' = 0.1\%\ \overline{\mathscr{E}_0}$. The reference frame is moving with velocity $c_{\text{ref}}=0.31$.

Orszag and Patera.[10] The vorticity q of the quasiequilibrium structure is nearly parallel to the streamfunction ψ in the interior of the flow, and further adjustments take place on a diffusion time scale $\sim R$. An elliptical vortex structure develops from the initial nearly parallel flow in less than 10 advective time units, which is considerably less than the time taken to reach the quasiequilibrium band from the finite amplitude Orr–Sommerfeld modes employed by Orszag and Patera. Further evidence that the finite amplitude solution is acting as an attractor in this flow follows from the observation that the mean velocity profile at time $t=200$, plotted in Fig. 6, is developing a small kink near each boundary similar to those of the finite amplitude solution.[6]

The evolution of the same optimal perturbation but with half the initial energy of the previous example ($0.05\%\ \overline{E_0}$) is shown in Fig. 7. The quasisteady elliptical vortex reached in less than ten advective time units for this perturbation is lower in amplitude than that in Fig. 3, but is clearly also attracted to the 2-D finite amplitude solution. If the initial energy is further reduced to $0.01\%\ \overline{E_0}$, however, the optimal perturbation does not have sufficient amplitude to develop into a quasiequilibrium state, and instead follows the linear pattern of energy growth followed by decay toward a laminar flow. For comparison with the rapid equilibration of the optimal perturbations, Fig. 8 shows the gradual decay of the least-damped Orr–Sommerfeld mode assigned an initial energy of $0.1\%\ \overline{E_0}$, equal to the initial energy for the optimal of Fig. 3 and near the modal threshold energy for quasiequilibria found by Orszag and Patera.

Figure 9 shows perturbation energy as a function of time for the four cases just described. It is interesting that the energy growth of the optimals at its first peak decreases as the initial assigned energy increases. When the initial energy is $0.1\%\ \overline{E_0}$ the energy peaks at $t\approx 14$ with energy growth by a factor of 19, compared to the optimal with $E_0=0.05\%\ \overline{E_0}$ which grows by 24 times and the optimal with $E_0=0.01\%\ \overline{E_0}$ which undergoes near linear energy growth by a factor of 31. The effect of nonlinearity here is to *limit* the potential for growth, which occurs through the linear mechanism of momentum transport through down-gradient Reynolds stress.

Finally, we consider whether the long-lasting elliptical vortices that have developed rapidly from sufficiently energetic optimal perturbations are capable of supporting secondary instabilities. Pierrehumbert[16] and Bayly[17] showed analytically that the secondary instability mechanism is possible for inviscid flow with locally elliptical streamlines. The analysis was extended to viscous flows by Landman and Saffman,[12] who determined a stability boundary in the Ekman number-eccentricity parameter plane. According to criteria derived from this stability boundary, the elliptical vortex in Fig. 3 at time $t=10$ is capable of sustaining 3-D secondary instability growth at an estimated growth rate of 0.02, such that order of magnitude energy growth occurs in 50 advective time units. However, the vortex resulting from $E_0'=0.05\%\ \overline{E_0}$ must develop further (on the viscous time scale) toward the 2-D finite amplitude solution before it is capable of supporting 3-D instabilities. This suggests a

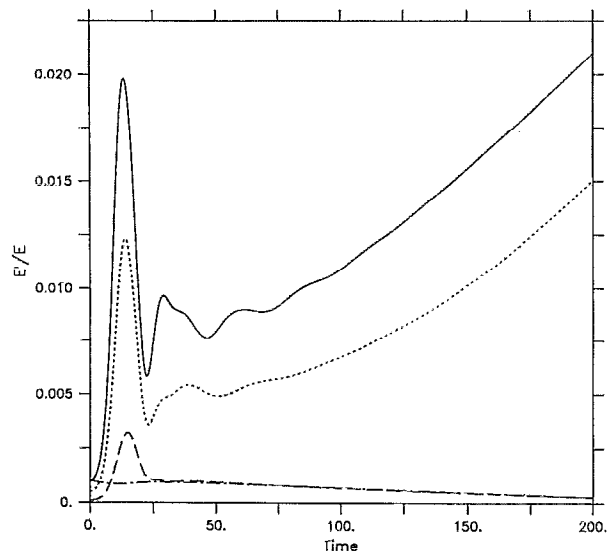

FIG. 9. Perturbation energy vs time for the evolution of energy optimals with $\mathscr{E}_0' = 0.1\%\ \overline{\mathscr{E}_0}$ (solid line), $\mathscr{E}_0' = 0.05\%\ \overline{\mathscr{E}_0}$ (dotted), and $\mathscr{E}_0' = 0.1\%\ \overline{\mathscr{E}_0}$ (dashed), and of the slowest-decaying Orr–Sommerfeld mode with $\mathscr{E}_0' = 0.01\%\ \overline{\mathscr{E}_0}$ (dot–dash) in Poiseuille flow.

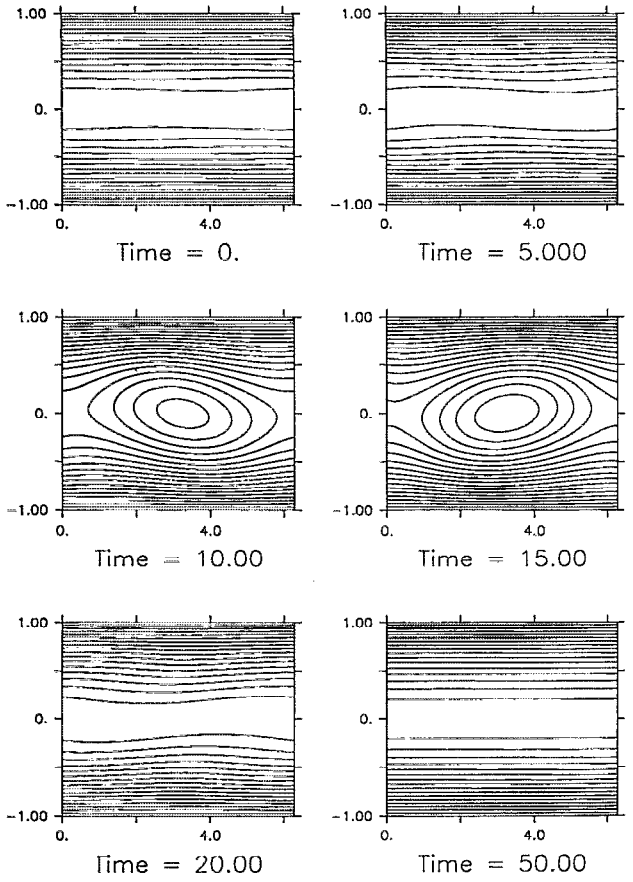

FIG. 10. Evolution of the total streamfunction for the 2-D energy optimal in Couette flow with $R=2000$, $\alpha=1.0$, $\tau=13$, and initial perturbation energy $\mathscr{E}_0' = 0.1\%\ \overline{\mathscr{E}_0}$, showing the rapid growth and just as rapid decay of an elliptical vortex starting from nearly parallel flow. The reference frame is moving with velocity $c_{ref}=0$.

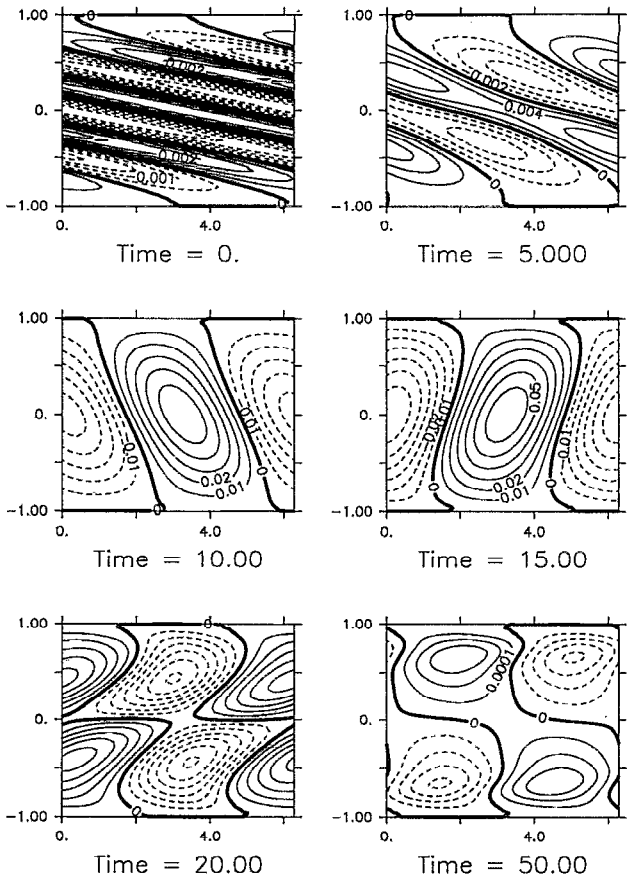

FIG. 11. Evolution of the perturbation streamfunction for the flow in Fig. 10.

threshold initial perturbation energy on the order of 0.1% of the mean energy for rapid (advective time scale) development of secondary instability from a nearly parallel background flow.

V. COUETTE FLOW

Unlike Poiseuille flow, Couette flow is linearly stable to infinitesimal disturbances at finite Reynolds numbers, and there are no known finite amplitude 2-D solutions. However, the least stable Orr–Sommerfeld (OS) mode is slowly-decaying for high Reynolds numbers, so it may be possible to locate regions of quasiequilibria that tend to attract properly configured initial conditions. Orszag and Patera[8] were able to observe growth of three-dimensional secondary instabilities on slowest-decaying OS modes of finite amplitude for Reynolds numbers down to $R\approx1000$. In this section, we study the potential of optimal perturbations with small initial energies to develop into finite amplitude quasiequilibrium structures in Couette flow.

The first initial condition to be studied is the energy optimal, which in the case of Poiseuille flow resulted in the finite amplitude equilibrium structure. The Reynolds number chosen is $R=2000$, above a value ($R=1500$) at which Orszag and Patera[10] were able to sustain secondary instabilities on the slowest-decaying Orr-Sommerfeld mode with initial energy $E_0' = 4\%\ \overline{E_0}$. The initial perturbation chosen is the two-dimensional disturbance which gains close to the maximum energy under linear conditions at this Reynolds number, with wave number $\alpha=1.0$, energy growth period $\tau=13$, and maximum linear energy growth of $E_\tau/E_0=20.3$.

The total streamfunction showing the nonlinear evolution of this optimal perturbation from an initial energy $E_0' = 0.1\%\ \overline{E_0}$, (Fig. 10), shows the failure of this choice to develop into a quasiequilibrium state. Instead, the disturbance follows the same path of rapid transient growth and decay observed for infinitesimal optimal disturbances. The evolution of the perturbation streamfunction in time is shown in Fig. 11.

Comparison with the development of the energy optimal in Poiseuille flow suggests that the energy optimal for Couette flow fails to equilibrate because no nearby 2-D solution or quasiequilibrium state exists to serve as an attractor for this flow, which is symmetric about the centerline. The optimal perturbation that feeds the most energy into the (asymmetric) slowest-decaying mode may therefore be a more promising initial condition for development into a long-lived nonlinear structure. This modal optimal, assigned an initial energy of $E_0' = 0.1\%\ \overline{E_0}$, was found to perform little better than the energy optimal, decaying to a nearly

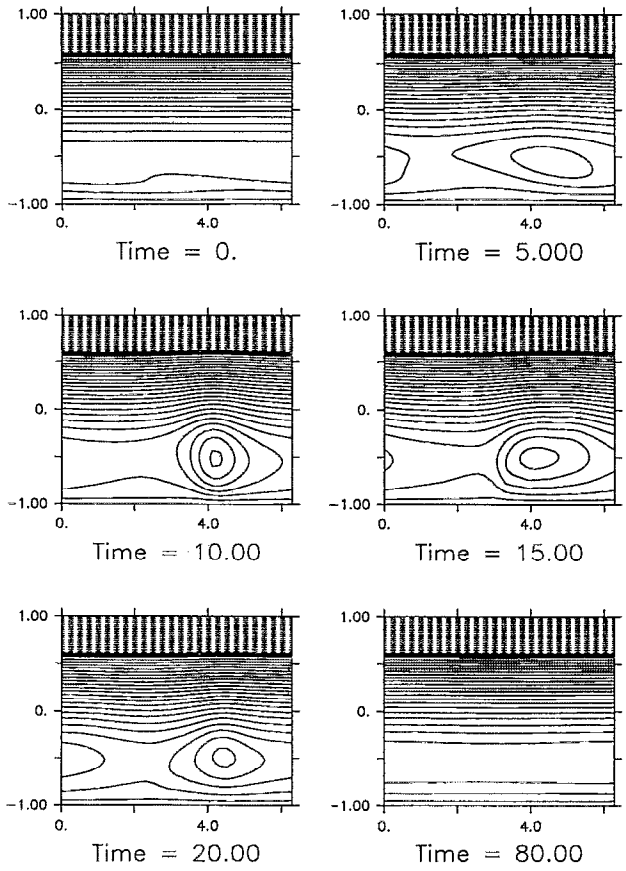

FIG. 12. Evolution of the total streamfunction for the optimal in Couette flow that feeds most energy into the slowest-decaying Orr–Sommerfeld mode, with $R=2000$, $\alpha=1.0$, and initial perturbation energy $\mathscr{E}_0' = 0.5\%\ \overline{\mathscr{E}_0}$. The reference frame is moving with velocity $c_{\text{ref}}=-0.55$.

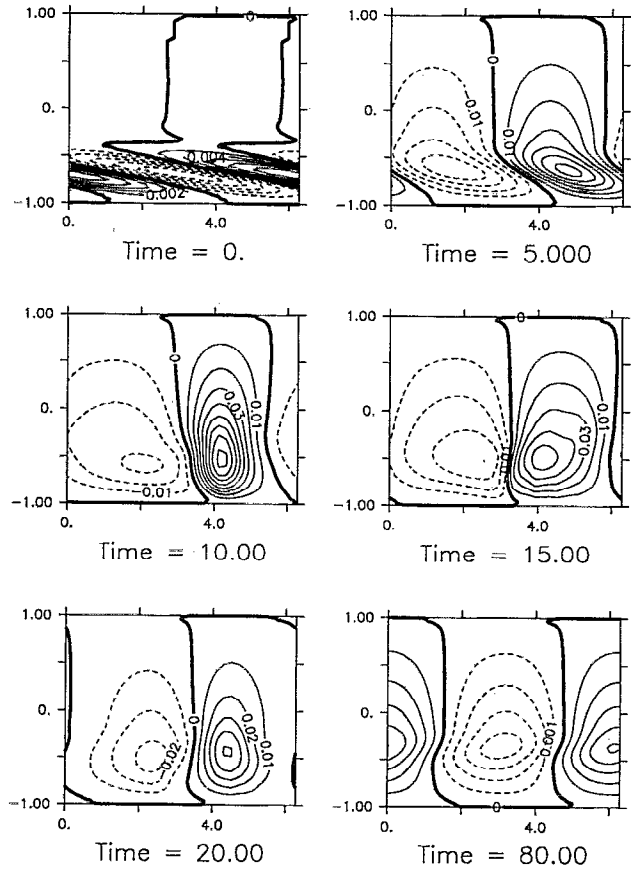

FIG. 13. Evolution of the perturbation streamfunction for the flow in Fig. 12.

parallel flow by $t=30$. Figures 12 and 13 show the evolution of the modal optimal with a larger initial energy of $E_0' = 0.5\%\ \overline{E_0}$. This perturbation is able to sustain a finite amplitude elliptical vortex for a longer time period than the previous attempts primarily because the decay of this mode-like disturbance proceeds from a larger initial amplitude.

Figure 14 displays the perturbation energy versus time from the above initial conditions of energy and modal optimals, along with an imposed Orr–Sommerfeld mode with $E_0'=0.5\%\ \overline{E_0}$.

This failure of large amplitude optimal disturbances in a constant shear flow to exhibit nonlinear behavior is in agreement with the result of Tung[18] that if the initial nonlinear terms of a bounded disturbance in uniform shear flow are small, then they will remain small for all time.

VI. LOCAL INSTABILITIES FOR QUASIEQUILIBRIUM STRUCTURE

Frequent reference is made in the viscous shear flow literature[19] to the stability properties of flow profiles that are inflectional in some local region. These profiles are thought to be significant because of Rayleigh's inflection-point-theorem,[20] which states that an inflection point is a necessary condition for instability of an inviscid shear flow. Because certain inflectional flows are strongly unstable (on an advective time scale), it is often assumed that a locally inflectional flow is a good candidate for growth of secondary instabilities. In this section, we explore this idea for the quasiequilibrium flow state from Sec. IV.

Figure 15 shows the local velocity profiles at eight x locations separated by $\Delta x=a/16$ for the quasiequilibrium structure in Poiseuille flow with $R=4000$ at $t=200$ (see Fig. 5). Clearly each of these flows has at least one inflection point.

The wave number for the most unstable eigenmode of each local profile and of the mean profile $\bar{u}$ (Fig. 6) is listed in Table I along with the corresponding wave speed c_r and growth rate αc_i. Note that some local profiles are stable despite the existence of inflection points. The growth rates of the unstable modes are slow, and the cutoff wave numbers α_0, above which no growing mode was found for the unstable profiles in Table I, indicate that the wavelengths of unstable modes are larger than the local region described by each profile.

VII. DISCUSSION

2-D perturbations that are favorably configured for transient energy growth in viscous shear flow have been shown in this work to rapidly develop into quasisteady finite amplitude structures under conditions of (a) sufficient initial am-

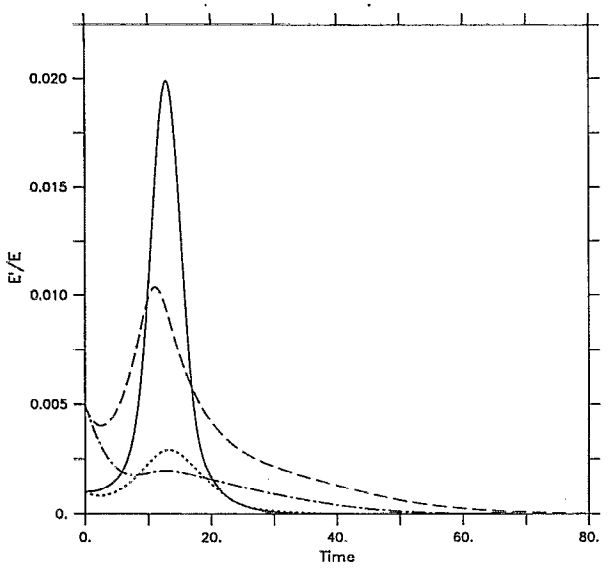

FIG. 14. Perturbation energy versus time for the energy optimal with $\mathscr{E}_0' = 0.1\%\ \overline{\mathscr{E}_0}$ (solid line), modal optimals with $\mathscr{E}_0' = 0.5\%\ \overline{\mathscr{E}_0}$ (dashed), and $\mathscr{E}_0' = 0.1\%\ \overline{\mathscr{E}_0}$ (dotted) and the slowest-decaying Orr–Sommerfeld mode with $\mathscr{E}_0' = 0.5\%\ \overline{\mathscr{E}_0}$ (dot–dash) in Couette flow.

plitude, and (b) the existence of a nearby finite amplitude nonlinear mode or quasimode. The rapid growth of these disturbances is due to the down-gradient transport of mean momentum by the Reynolds stress, as indicated by the initial orientation of the perturbation streamlines in the direction opposite the shear. (The same linear mechanism operates for shear instability, although there are no unstable modes at the Reynolds numbers examined in this work.)

Optimal perturbations are found to develop rapidly into persistent 2-D finite amplitude structures from initial conditions with energy densities on the order of 0.1% of the mean

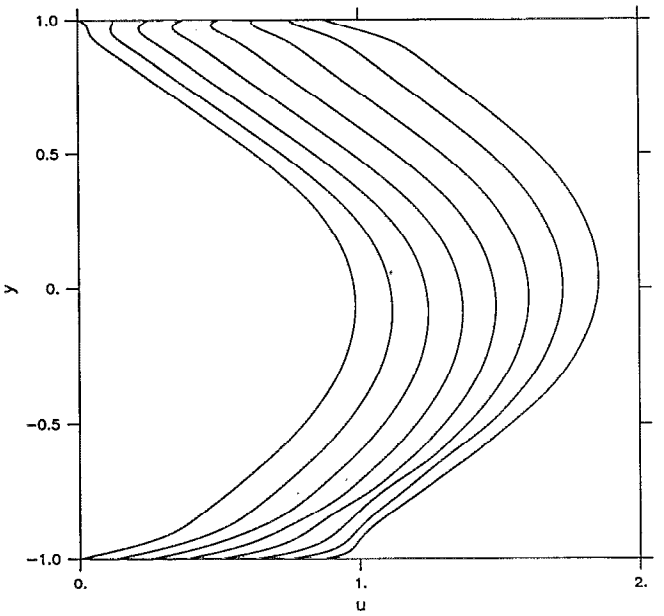

FIG. 15. Streamwise velocity u profiles at intervals of $\Delta x = \pi/8\alpha$ for the Poiseuille flow quasiequilibrium at $t=200$ (see Fig. 5) illustrating locally inflectional profiles.

TABLE I. Stability properties of local profiles for an equilibrated flow field (see Fig. 15).

Profile #	$\alpha_{\max}$	$c_{r\ \max}$	$\alpha c_{i\ \max}$	α_0
1	0.80	0.27	+0.0045	0.9
2	0.65	0.24	−0.0026	···
3	0.65	0.23	−0.0064	···
4	0.75	0.24	−0.0027	···
5	0.90	0.29	+0.0083	1.7
6	2.1	0.51	+0.074	4.1
7	1.15	0.38	+0.028	1.6
8	1.05	0.33	+0.027	1.3
$\bar{u}$	1.00	0.33	−0.0019	···

flow energy density for Poiseuille flow and 1% of the mean flow energy density for Couette flow. It should be emphasized, however, that 3-D optimal perturbations are capable of energy growth two orders of magnitude greater than the 2-D optimals, as shown by Gustavsson[21] and Butler and Farrell.[22] This suggests that 3-D disturbances are more likely to appear in a natural flow field and dominate the flow throughout the transition process.

The inability of locally inflectional velocity profiles of a sample quasiequilibrium structure to support strongly growing eigenmodes suggests caution in the assumption that the necessary Rayleigh condition is sufficient to explain observations of secondary instability and flow breakdown. This conclusion is supported by recent research on the breakdown of streamwise vortices by Swearingen and Blackwelder[23] and Hamilton.[24]

ACKNOWLEDGMENTS

This work was supported by NSF ATM-8912432, with computer time provided by NCSA ATM-900015N and NCAR 35121031. The National Center for Atmospheric Research is supported by the National Science Foundation. Support for K. Butler from the Zonta International Amelia Earhart Fellowship and the Robert L. Wallace Prize Fellowship is also gratefully acknowledged.

[1]P. S. Klebanoff, K. D. Tidstrom, and L. M. Sargent, "The three-dimensional nature of boundary-layer instability," J. Fluid Mech. **12**, 1 (1962).
[2]M. Nishioka, S. Iida, and Y. Ichikawa, "An experimental investigation of the stability of plane Poiseuille flow," J. Fluid Mech. **72**, 731 (1975).
[3]B. J. Bayly, S. A. Orszag, and T. Herbert, "Instability mechanisms in shear-flow transition," Annu. Rev. Fluid Mech. **20**, 359 (1988).
[4]T. Herbert, "Secondary instability of boundary layers," Annu. Rev. Fluid Mech. **20**, 487 (1988).
[5]S. A. Orszag, "Accurate solution of the Orr–Sommerfeld stability equation," J. Fluid Mech. **50**, 689 (1971).
[6]J.-P. Zahn, J. Toomre, E. A. Spiegel, and D. O. Gough, "Nonlinear cellular motions in Poiseuille channel flow," J. Fluid Mech. **64**, 319 (1974).
[7]T. Herbert, "Periodic secondary motions in a plane channel," in *Proceedings of the Fifth International Conference on Numerical Methods in Fluid Dynamics*, Lecture Notes in Physics No. 59, edited by A. I. van de Vooren and P. J. Zandbergen (Springer-Verlag, Berlin, 1976), Vol. 59, p. 235.
[8]S. A. Orszag and A. T. Patera, "Subcritical transition to turbulence in plane channel flows," Phys. Rev. Lett. **45**, 989 (1980).
[9]M. Nagata, "Three-dimensional finite-amplitude solutions in plane Couette flow: Bifurcation from infinity," J. Fluid Mech. **217**, 519 (1990).
[10]S. A. Orszag and A. T. Patera, "Subcritical transition to turbulence in

planar shear flows," in *Transition and Turbulence*, edited by R. E. Meyer (Academic, New York, 1981), p. 127.
[11]B. F. Farrell, "Optimal excitation of perturbations in viscous shear flow," Phys. Fluids **31**, 2093 (1988).
[12]M. J. Landman and P. G. Saffman, "The three-dimensional instability of strained vortices in a viscous fluid," Phys. Fluids **30**, 2339 (1987).
[13]C. C. Lin, "Some mathematical problems in the theory of the stability of parallel flows," J. Fluid Mech. **10**, 430 (1961).
[14]I. V. Schensted, "Contributions to the theory of hydrodynamic stability," Ph.D. thesis, University of Michigan, 1960.
[15]R. C. DiPrima and G. J. Habetler, "A completeness theorem for nonself-adjoint eigenvalue problems in hydrodynamic stability," Arch. Rat. Mech. Anal. **34**, 218 (1969).
[16]R. T. Pierrehumbert, "Universal short-wave instability of two-dimensional eddies in an inviscid fluid," Phys. Rev. Lett. **57**, 2157 (1986).
[17]B. J. Bayly, "Three-dimensional instability of elliptical flow," Phys. Rev. Lett. **57**, 2160 (1986).
[18]K. K. Tung, "Initial-value problems for Rossby waves in a shear flow with critical level," J. Fluid Mech. **133**, 443 (1983).
[19]D. R. Williams, H. Fasel, and F. R. Hama, "Experimental determination of the three-dimensional vorticity field in the boundary-layer transition process," J. Fluid Mech. **149**, 179 (1984).
[20]Lord Rayleigh, "On the stability, or instability, of certain fluid motions," Proc. London Math. Soc. **11**, 57 (1880).
[21]L. H. Gustavsson, "Energy growth of three-dimensional disturbances in plane Poiseuille flow," J. Fluid Mech. **224**, 241 (1991).
[22]K. M. Butler and B. F. Farrell, "Three-dimensional optimal perturbations in viscous shear flow," Phys. Fluids A **4**, 1637 (1992).
[23]J. D. Swearingen and R. F. Blackwelder, "The growth and breakdown of streamwise vortices in the presence of a wall," J. Fluid Mech. **182**, 255 (1987).
[24]J. M. Hamilton, "Streamwise vortices and transition to turbulence," Ph.D. thesis, Harvard University, 1991.